

Contents lists available at [SciVerse ScienceDirect](http://www.sciencedirect.com)

Biomaterials

journal homepage: www.elsevier.com/locate/biomaterials

Anti-leukemia activity of PVP-coated silver nanoparticles via generation of reactive oxygen species and release of silver ions

Dawei Guo^{a,b}, Lingying Zhu^{a,b}, Zhihai Huang^{a,b}, Haixia Zhou^c, Yue Ge^d, Wenjuan Ma^d, Jie Wu^d, Xiuyan Zhang^d, Xuefeng Zhou^{a,b}, Yu Zhang^a, Yun Zhao^{d,*,1}, Ning Gu^{a,b,*,1}

^aState Key Laboratory of Bioelectronics, Jiangsu Key Laboratory for Biomaterials and Devices, School of Biological Science and Medical Engineering, Southeast University, Nanjing 210096, PR China

^bSuzhou Key Laboratory of Biomedical Materials and Technology, Research Institute of Southeast University in Suzhou, Suzhou 215123, PR China

^cThe First Affiliated Hospital, Jiangsu Institute of Hematology, Soochow University, Suzhou 215006, PR China

^dCyrus Tang Hematology Center, Soochow University, 199 Ren'ai Road, Suzhou 215123, PR China

ARTICLE INFO

Article history:

Received 10 May 2013

Accepted 3 July 2013

Available online xxx

Keywords:

Silver nanoparticles
Acute myeloid leukemia
Cytotoxicity
Reactive oxygen species
Silver ions

ABSTRACT

Silver nanoparticles (AgNPs) have anti-cancer effect. However, whether and how these particles could inhibit the growth of acute myeloid leukemia (AML) cells is unclear. In the present study, we prepared AgNPs with various sizes and investigated their cytotoxic effect on AML cells. We found that AgNPs could inhibit the viability of AML cells including the isolates from AML patients. AgNPs caused the production of reactive oxygen species (ROS), losses of mitochondrial membrane potential (MMP), DNA damage and apoptosis. Both vitamin C (Vit C) and N-acetyl-L-cysteine (NAC) could completely reverse the generation of ROS upon AgNPs, however only NAC but not Vit C could protect the cells from losses of MMP, DNA damage and apoptosis thoroughly. Similar results were obtained when cells were treated with silver ions alone. As NAC was not only an antioxidant to scavenge ROS but also a silver ion chelator, these data supported the model that both generation of ROS and release of silver ions played critical roles in the AgNPs-induced cytotoxic effect against AML cells. Taken together, this work elucidated the cytotoxic effect of AgNPs on AML cells and their underlying mechanism and might have significant impact on AML treatment.

© 2013 Elsevier Ltd. All rights reserved.

1. Introduction

Acute myeloid leukemia (AML) is a clonal disease characterized by the proliferation and accumulation of immature myeloid cells in the bone marrow, which ultimately leads to hematopoietic failure [1]. AML is heterogeneous disease consisting of multiple subtypes (M0–M7) classified with the French–American–British (FAB) criteria based on the morphologic and cytochemical features of leukemic cells [2]. These days AML therapy is based upon the principles of combination of multiple effective agents, dose intensity, risk-adapted use of allogeneic hematopoietic stem cell transplantation, and improved supportive care. Extensive effort

was made to develop new agents for the treatment of AML, nevertheless the combination of AraC and anthracyclines is still the mainstay of induction therapy. Although several new agents have shown promise in treating AML, it is more likely that they will be used in combination with conventional therapy, but not administered as monotherapy [3].

Silver nanoparticles (AgNPs) have become the engineered nanomaterials with the highest degree of commercialization due to their broad-spectrum antimicrobial activities [4–6]. In addition, AgNPs have anti-fungi, anti-virus, anti-biofilm, anti-inflammation, anti-thrombosis effect, and enhance the healing of wounds [7–13]. AgNPs have also been explored as nanoprobe for the detection and imaging of tumors, vectors for drug delivery, as well as inhibitors to suppress angiogenesis and tumor growth [14–20]. Furthermore, several investigators have reported that AgNPs induced the cytotoxic effect against leukemic cells, such as THP-1, Jurkat and K562 cells [21–24], mainly through elevating reactive oxygen species (ROS); and these particles could also display a synergistic effect against leukemic cells with chemotherapeutic drugs, such as cyclophosphamide or busulfan [25].

* Corresponding author. State Key Laboratory of Bioelectronics, Jiangsu Key Laboratory for Biomaterials and Devices, School of Biological Science and Medical Engineering, Southeast University, 2 Sipailou, Nanjing 210096, PR China. Tel.: +86 25 83272460; fax: +86 25 83272476.

** Corresponding author. Tel.: +86 51 265880899x501; fax: +86 51 265880929.

E-mail addresses: zhaoy@suda.edu.cn (Y. Zhao), guning@seu.edu.cn (N. Gu).

¹ Ning Gu and Yun Zhao are co-senior authors.

Although there have been plenty of investigations to explore the potential application of AgNPs in cancer therapy using the cancer cell lines, however, there has been scarce investigation on the effect of AgNPs exposure on clinical isolates of cancer or leukemia [24]. It is thus of critical importance to understand the action of AgNPs on AML cells derived from various individuals prior to their therapeutic application. The toxicity of AgNPs has also been reported by a number of *in vitro* studies. It is well established that the chemical nature, size, surface chemistry, their ability to bind and affect biological sites as well as their metabolism and excretion have been deemed important properties influencing NP-mediated toxicity [26–29]. However, the mechanism underlying AgNPs-induced biological effects has not been clearly elucidated, especially there has been no conclusive answer to address whether the AgNPs-mediated cytotoxicity originate primarily from silver nanoparticles or silver ions released from particles, or the combination of both [30–33].

In the present study, we successfully prepared PVP-coated AgNPs with three sizes using an electrochemical method, and studied their biological effects on cell lines and clinical isolates from AML patients. Our results showed that AgNPs could effectively reduce cell viability via generation of reactive oxygen species (ROS) and release of silver ions, and ultimately led to DNA damage and apoptosis. Taken together, this study illustrated the cytotoxicity against AML cells induced by PVP-coated AgNPs and their underlying mechanisms, which provided evidences to promote the application of AgNPs in the treatment of AML.

2. Materials and methods

2.1. Synthesis of silver nanoparticles

In the current study, silver nanoparticles (AgNPs) were synthesized by a continuous flow electrochemical process as reported previously [34], in which polyvinylpyrrolidone (PVP) and two silver rods were used as the stable agent and electrodes, respectively. PVP was of analytical grade and used without further purification, and the purity of the silver rods was 99.99%. The synthesis process was typically described as follows. Firstly, the silver electrodes were polished with ultrafine carborundum paper, and then were fitted on the reactor's cover after washing with absolute ethyl alcohol. Secondly, the electrolytic solution containing PVP of 5 mg/ml was prepared and filled into the syringe. The reaction temperature was kept at 60 °C. Subsequently, the electrolytic solution was continuously injected into reactor through the inlet tube of the reactor's cover. The size of AgNPs was regulated by tuning the voltage and flow rate of electrolytic solution. During the reaction, the electrolytic solution was stirred with a magnetic rotor, and the current direction of the electrodes was alternatively changed every minute. After the reactor was filled, the product flowed out from outlet tube of the reactor's cover. Finally, the freeze-dried powders of AgNPs were obtained after filtration, centrifugation and lyophilization.

2.2. Characterization of silver nanoparticles

The synthesized nanoparticles were primarily characterized by UV–vis spectroscopy (Hitachi U-2000, Tokyo, Japan) followed by transmission electron microscopy (TEM, JEM-2000EX, JEOL, Japan). TEM samples were prepared by placing a few drops of their aqueous dispersions on carbon coated copper grids and drying at room temperature. The mean size was calculated from a random field of TEM images that showed the general morphology of nanoparticles. Over 200 particles were counted and measured to determine the mean sizes, standard deviations, and size distributions. The hydrodynamic diameters and zeta potentials of AgNPs were measured by dynamic light scattering (DLS) using a Zetasizer Nano ZS (Malvern Instruments, Worcestershire, UK). The final silver concentration in aqueous solution was determined by inductively coupled plasma mass spectrometry (ICP-MS).

2.3. Cell cultures

Acute myeloid leukemia cell lines (SHI-1, THP-1, DAMI, NB4, HL-60 and HEL cells) were cultured at 37 °C in an incubator with a humidified atmosphere of 5% CO₂ in RPMI 1640 (Hyclone, USA) supplied with 10% fetal bovine serum (FBS, Hyclone). The bone marrow aspirations of AML patients (the clinical characteristics summarized in Table 1) and healthy donors were collected with individual informed consent approved by the Ethical Committee of Soochow University from the First Affiliated Hospital of Soochow University, and then were purified with

Table 1

Clinical characteristics of the AML patients in this study.

Sample	Sex	Age	WBC ^a ($\times 10^9/L$)	Hb ^b (g/L)	Plt ^c ($\times 10^9/L$)	FAB ^d subtype
Pt#1	Male	73	174.99	100	27	M4
Pt#2	Male	32	30.78	95	10	M2
Pt#3	Male	50	207.82	97	10	M1
Pt#4	Male	67	0.65	55	28	M2
Pt#5	Female	20	91.6	78	49	M4
Pt#6	Male	46	45.2	63	20	M4
Pt#7	Female	59	1.59	105	81	M2
Pt#8	Female	17	2.11	76	45	M4
Pt#9	Female	34	0.96	69	11	M5
Pt#10	Male	43	75.58	58	22	M5
Pt#11	Male	37	10.28	95	89	M5

^a White blood cell.

^b Hemoglobin.

^c Platelet.

^d French–American–British.

^e Patient.

Ficoll–Hypaque (1.077 g/ml, GE Healthcare, US) following the manufacture's instruction. The nucleated cells were cultured in SFM (serum-free media) plus a cocktail of cytokines including SCF (stem cell factor, 100 ng/mL), FLT3 ligand (100 ng/mL), IL-3 (20 ng/mL), IL-6 (20 ng/mL) and G-CSF (20 ng/mL) overnight, and then all the experiments were done after 24 h treatment of AgNPs.

2.4. Cell viability assay

Cell viability was measured using CCK-8 assay (Cell Counting Kit-8, Beyotime, China) according to the manufacturer's instruction. Cells were seeded in 96 well microtitre plates (1×10^4 cells/200 μ l culture medium/well) with AgNPs at various concentrations. 24 h later, CCK-8 reagent was added to each well and cells were incubated for 4 h, and then the absorbance at two wavelengths (450 nm for soluble dye and 650 nm for viable cells) was detected using a microplate reader (SpectraMax M5, Molecular Devices, Sunnyvale, CA, USA). The cells treated with AgNPs were the experimental measurements (Read A), at the same time media plus AgNPs were used as the condition controls (Read B). The cells untreated with AgNPs were used as the negative control (Read C). The effect of nanoparticles on cells was expressed as the percentage of cell viability calculated as the following formula: Cell viability (%) = $(A - B)/(C - B) \times 100\%$. IC50 of each sample was calculated with GraphPad Prism (version 5.0).

2.5. Reactive oxygen species generation

To measure the intracellular generation of reactive oxygen species (ROS), SHI-1 cells were loaded with fluorescent marker 10 μ M 2',7'-dichlorodihydrofluorescein diacetate (H₂DCF-DA, Sigma, US) in RPMI 1640 without phenol red for 30 min and then washed with PBS and re-suspended in RPMI 1640 without phenol red. Cells were exposed to AgNPs at various concentrations for 3 h in the dark (37 °C, 5% CO₂) and immediately analyzed with flow cytometry (Calibur™, Becton–Dickinson). The 488 nm laser was used for excitation and fluorescence was detected in FL-1 by a 525/30 BP filter. For each sample, the mean fluorescence intensity of 10,000 cells was determined to present its intracellular production of ROS.

2.6. Mitochondrial membrane potential analysis

The mitochondrial membrane potential (MMP) was investigated using the fluorescent lipophilic cationic dye JC-1 (Beyotime, China). This dye reagent easily enters the mitochondria, aggregates, and fluoresces red. When MMP collapses, the dye reagent can no longer accumulate within the mitochondria and fluoresce green. Briefly, SHI-1 cells were pretreated with the antioxidants (Vit C or NAC) for 1 h prior to AgNPs-treatment for 24 h. The cells were incubated at 37 °C for 20 min with JC-1, washed twice with PBS and then placed in RPMI 1640 without phenol red. The red fluorescence intensity of stained cells was assayed using flow cytometry (Calibur™, BD).

2.7. Apoptosis assay

For Annexin V-FLUOS/propidium iodide (PI) assays, cells were stained and analyzed for apoptosis with flow cytometry according to the manufacturer's protocol. Briefly, 1×10^5 cells were stained with incubation buffer consisting of 2 μ l Annexin V-FLUOS and 2 μ l PI for 20 min at room temperature in dark. The apoptotic/necrotic cells were analyzed with flow cytometry.

2.8. DNA damage assay

After exposure to AgNPs for 24 h, cells were washed with PBS, deposited on a slide, and fixed with 4% formaldehyde in PBS for 15 min. The cells were blocked in

blocking buffer ($1 \times$ PBS/5% normal goat serum/0.3% Triton X-100) for 60 min, and then incubated with Alexa Fluor[®] 488 Conjugated Phospho-Histone H2A.X rabbit mAb (Cell Signaling Technology) overnight at 4 °C. Hoechst 33342 was used to stain the nuclei. Prolong[®] Gold Anti-Fade Reagent (Life Technologies) was used to mount the coverslip before the images were acquired with confocal microscopy (FV1000MPE-share, Olympus, Japan).

2.9. Statistical analysis

Statistical analysis of the obtained data was performed using SPSS software (version 16.0) and all values were represented as the means \pm SD of more than three independent experiments. The results were subjected to one-way ANOVA using the Duncan test to analyze the difference between the untreated and

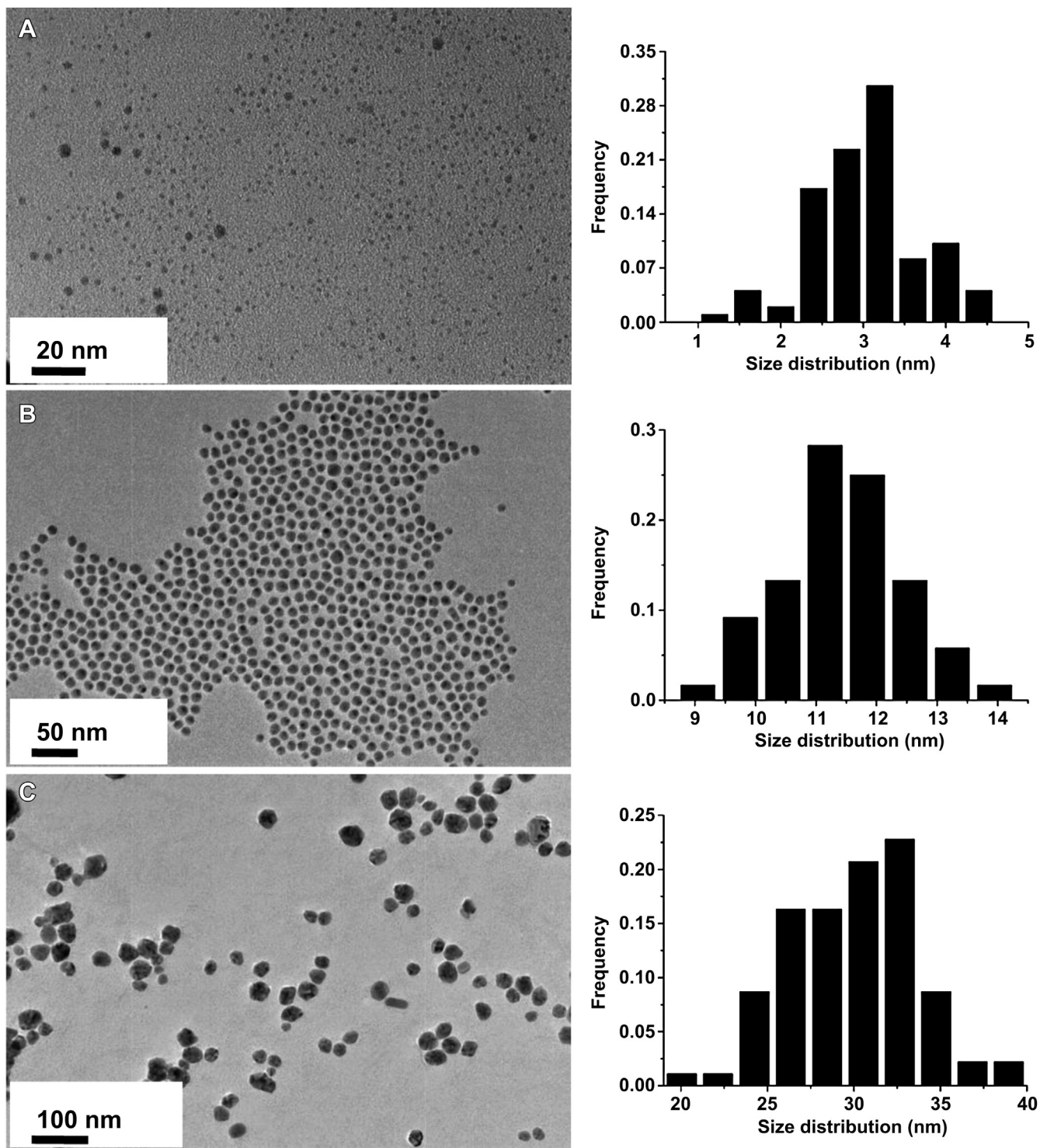


Fig. 1. The representative TEM images (Left) and size distribution histograms (Right) of silver nanoparticles (AgNPs). (A–C) The morphology of AgNPs was characterized by TEM and their size distribution histograms were obtained by size analysis of over 200 particles. The mean diameters were 2.92 ± 0.22 nm, 11.17 ± 0.62 nm, and 29.86 ± 0.52 nm, respectively. Scale bars were 20 nm, 50 nm and 100 nm, respectively.

untreated groups, in which a *P*-value less than 0.05 was considered as significant difference.

3. Results and discussion

3.1. Characterization of AgNPs

Due to the widespread applications of AgNPs, a large number of methods have been developed for the controllable synthesis of AgNPs, including physical, chemical and biological methods [6]. However, precise control on the size and distribution of AgNPs remains a great challenge [35]. In the current study, an electrochemical method was used to prepare uniform AgNPs of 3 nm (10 V, 100 mL/h), 11 nm (10 V, 80 mL/h) and 30 nm (15 V, 100 mL/h) by tuning the voltage and flow rate of electrolytic solution in the presence of poly(*N*-vinylpyrrolidone) (PVP) as a dispersant (Fig. 1). PVP has been widely utilized in medicine (e.g. as drug carrier, component of plasma substitute or wound dressing) due to its hemocompatible and physiologically inactive properties [36–38]. PVP is one of the most commonly applied stabilizers and protective agents for AgNPs synthesis [39]. PVP playing a role in AgNPs formation has been described by many studies. Overall, PVP not only effectively stabilizes AgNPs and but also promotes the nucleation of AgNPs [39,40].

Transmission electron microscopy (TEM) analysis revealed that as-prepared AgNPs in the present study were in approximately spherical shape and quite uniform (Fig. 1). The mean sizes of these AgNPs were 2.92 ± 0.22 nm (Fig. 1A), 11.17 ± 0.62 nm (Fig. 1B), and 29.86 ± 0.52 nm (Fig. 1C), respectively, which were statistically obtained by analysis of the recorded TEM images. The UV–vis spectroscopy has been proved to be a very useful technique for the analysis of nanoparticles. The UV–vis absorption spectra of AgNPs with three sizes displayed various maximum absorption wavelength, which were 421 nm for 3 nm AgNPs, 393 nm for 11 nm AgNPs, and 406.5 nm for 30 nm AgNPs, respectively (Fig. 2). The dominating feature in the optical spectra of AgNPs is usually the surface plasmon resonance (SPR), which can be described by the classical Mie theory. The resonance position and the peak width depend on many factors and gain insight into several physical properties of AgNPs. The SPR peaks of AgNPs displayed a continuous red-shift with the increasing sizes of the as-prepared AgNPs [35]. Therefore, the wavelength of maximum absorption peak of 30 nm AgNP showed a red-shift compared with that of 11 nm

AgNPs. For small silver clusters (<10 nm), the Mie theory predicts almost no influence of the cluster size on the position of the resonance, which is located around 350 nm for small spherical Ag clusters in vacuum (calculated from Mie theory). However, already small changes in the electronic properties of the surrounding medium of the cluster lead to strong shifts of the peak, and the width increases with decreasing cluster size due to additional scattering processes of the oscillating electrons at the cluster surface [41]. Therefore, the wavelength of maximum absorption peak of 3 nm AgNPs displayed a red-shift compared with that of 11 nm AgNPs and 30 nm AgNPs, and the absorbance peak was also broader (Fig. 2). A broader SPR peak indicated a broader size distribution, which was confirmed by the hydrodynamic diameters and the higher polydispersity index (PDI) from DLS (Table 2). Although the TEM image of 3 nm AgNPs showed the smaller size and distribution, there was no significant difference between hydrodynamic diameters of 3 nm AgNPs and 11 nm AgNPs.

3.2. Effect of AgNPs on cell viability

The cells from various organs or tissues usually display the differential susceptibility to AgNPs [22,26]. Herein, 6 AML cell lines (NB4, HL-60, SHI-1, THP-1, HEL and DAMI cells) were used to study their sensitivity to AgNPs by CCK-8 assay. AgNPs with various sizes reduced cell viability in a dose-dependent manner after 24 h incubation in all AML cell lines. However, various cell lines appeared to exhibit the heterogeneous sensitivity to the toxic effect of AgNPs. Moreover, the results revealed that THP-1 cells showed the most significant reduction in cell viability whereas SHI-1 cells were least sensitive to cytotoxic effects of AgNPs although both of them generated from patients with M5 (Fig. 3), suggesting that the sensitivity to AgNPs could not be concluded according to the FAB classification. It was reported that both the size and surface area played critical roles in nanoparticle cytotoxicity [42]. Based on the fact that the smaller nanoparticles usually have the bigger surface area and higher reactivity [43], the smaller was the size of AgNPs the stronger cytotoxic effect they could have, which was consistent with the comparison between 11 nm AgNPs and 30 nm AgNPs (Fig. 3). However, the size-dependent effect was not found between 3 nm AgNPs and 11 nm AgNPs due to the fact that their hydrodynamic diameters were not significantly different, which suggested that the stability of nanoparticles in aqueous solution was critical for nanotoxicity as well. All these results presented above indicated that the size and dose of AgNPs and cells used in the test played important roles in the cytotoxicity of AgNPs. Taken the stability and activity of NPs with various sizes into account, 11 nm AgNPs was used in the subsequent studies.

In vitro evaluation of AgNPs-mediated cytotoxicity can give an indicator of the toxicity *in vivo*. Currently, in most of studies the cytotoxicity of AgNPs was assessed using cultured cell lines [4,29]. Although established cell lines have been used in the toxicity screening as well as for studies of the toxic mechanism, excessive subculture could disturb the properties of some cultured cells over time [44]. The cultured primary cells appear to be the most powerful system for the *in vitro* new drug screening and toxicity evaluation [45]. Therefore, the primary cells of AML patients were

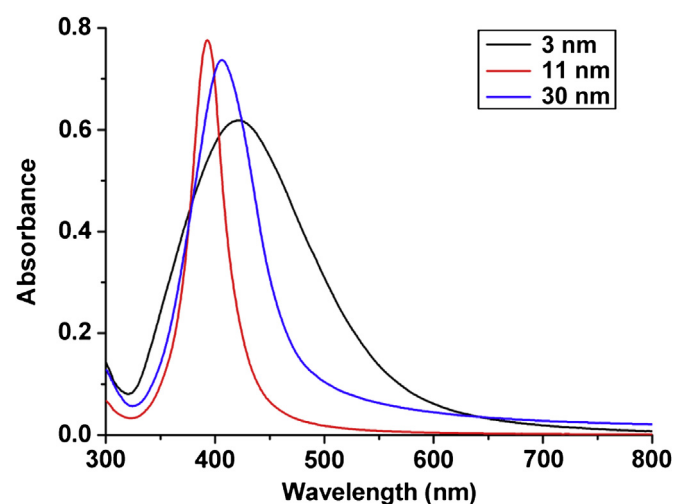


Fig. 2. The UV–vis absorption spectra of AgNPs with various sizes. The wavelength of maximum absorption peak was 421 nm for 3 nm AgNPs, 393 nm for 11 nm AgNPs and 406.5 nm for 30 nm AgNPs, respectively.

Table 2
Hydrodynamic diameters and zeta potentials of AgNPs.

Sample	Z-average (d nm)	Polydispersity index (PDI)	Zeta potential (mV)
AgNPs-3 nm	27.84 ± 0.1966	0.546 ± 0.231	-12.5 ± 1.20
AgNPs-11 nm	33.52 ± 0.6658	0.365 ± 0.045	-16.4 ± 1.36
AgNPs-30 nm	61.47 ± 0.6995	0.288 ± 0.027	-19.7 ± 0.60

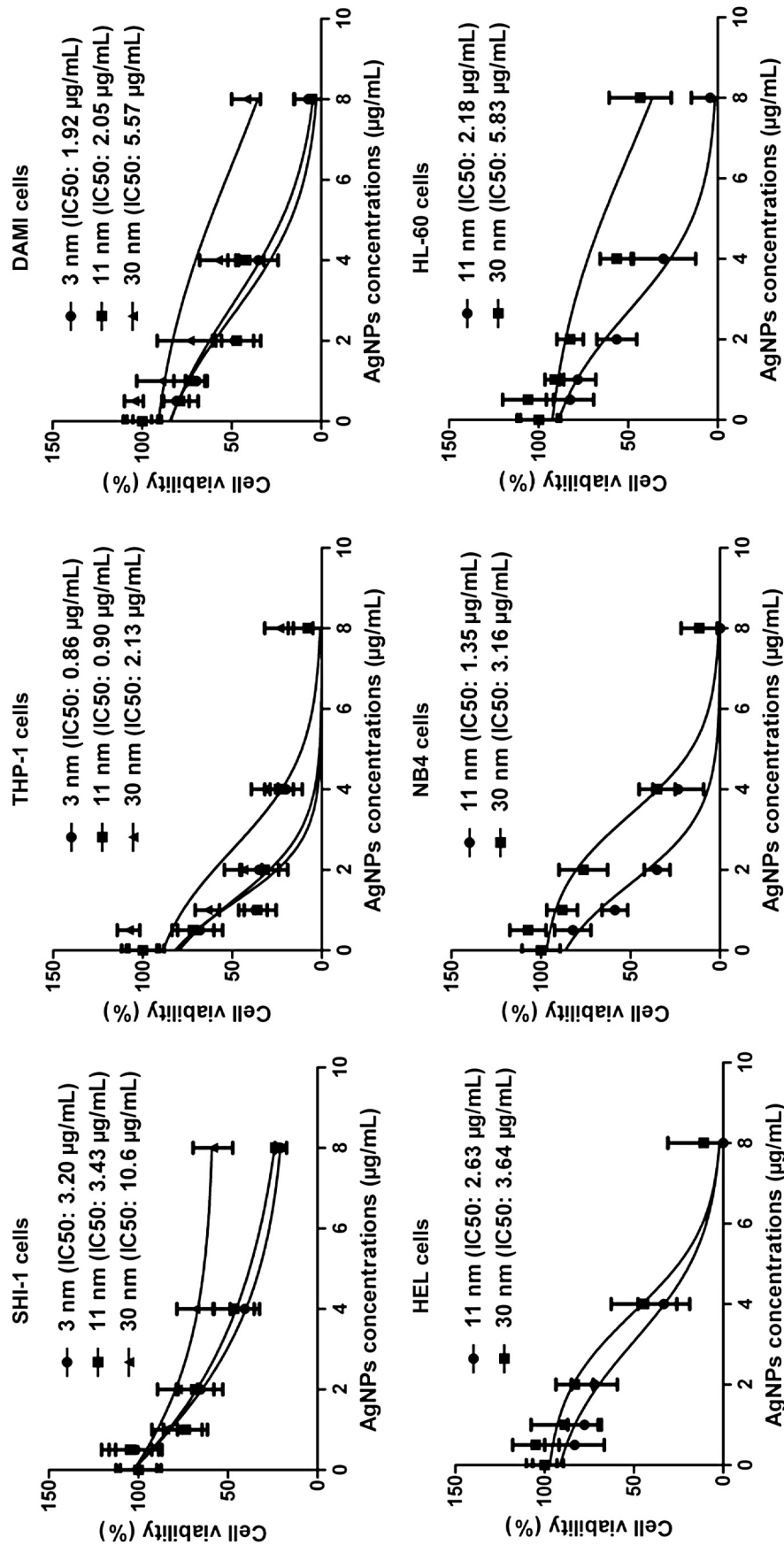


Fig. 3. Effect of AgNPs with various sizes on the viability of AML cell lines. The viability of various AML cell lines was determined 24 h after treatment with AgNPs at various concentrations.

collected, and their viability was studied upon exposure of AgNPs. As described in Fig. 4, AgNPs decreased the viability of clinical isolates of AML patients in a dose-dependent manner and the various patient-derived cells had differential sensitivity to AgNPs, which was consistent with the results of the AML cell lines. Overall, there was not significant difference in the sensitivity upon AgNPs between the clinical isolates from AML patients and cells from healthy donors due to their similar IC50. However, AgNPs at lower concentration but not at high concentrations had stronger cytotoxic effect against the isolates from AML patients than that towards cells from healthy donors, which was similar to our previous report that the cells derived from a subset of chronic myeloid leukemia (CML) patients were more sensitive to AgNPs at lower concentrations compared to the normal control [24].

3.3. Generation of reactive oxygen species after exposure to AgNPs

It is reported that oxidative stress is one of the critical mechanisms of cytotoxicity induced by AgNPs [21,27,46,47]. Increased intracellular reactive oxygen species (ROS) will perturb the redox potential equilibrium, bring about an intracellular pro-oxidant environment and ultimately result in a series of adverse biological effects. In the current study, AgNPs could stimulate ROS production in a dose-dependent manner. Compared to the untreated cells, those treated with AgNPs at 8 $\mu\text{g}/\text{mL}$ had 3-fold increase of ROS, which could be completely prevented by pretreatment with the antioxidant agents, such as Vit C (50 μM) or NAC (5 mM) (Fig. 5).

3.4. Mitochondrial damage induced by AgNPs

It was further investigated whether ROS generation induced by AgNPs was involved with mitochondrial membrane potential (MMP) changes. It is well-known that mitochondria are the major sites of ROS production inside cells. Excess ROS generation can result in mitochondrial damage, which in turn leads to uncontrolled ROS formation. Mitochondria damage leads to the dissipation of MMP, which is an indicator of the impaired mitochondrial integrity. MMP can be investigated using the fluorescent lipophilic cationic dye JC-1 [27], as this dye could easily enter the mitochondria, aggregate, and fluoresce red. When MMP collapses, the dye reagent can no longer accumulate within the mitochondria and fluoresce green. As observed in Fig. 6, the intensity of intracellular

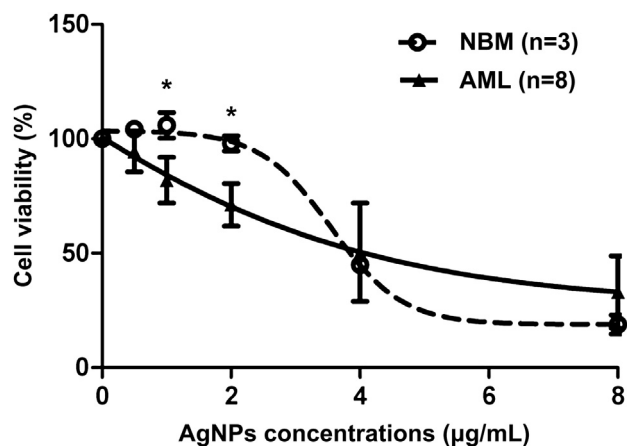


Fig. 4. Effect of AgNPs (11 nm) on the viability of isolates from AML patients and healthy donors. The viability of cells from the AML patients and healthy donors was determined 24 h after AgNPs treatment. IC50 of AgNPs against the primary cells from the AML patients and healthy donors was 4.21 and 4.05 $\mu\text{g}/\text{mL}$, respectively. * denoted significant difference ($P < 0.05$) between AML patients and healthy donors at the same concentration.

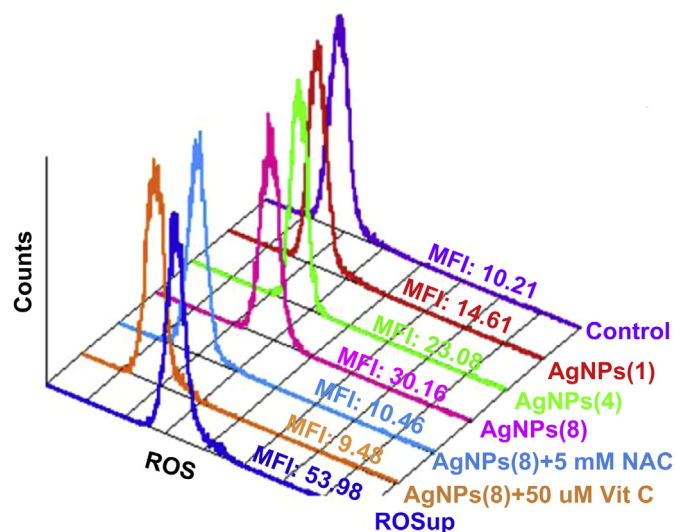


Fig. 5. Generation of ROS in SHI-1 cells exposed to AgNPs (11 nm) at various concentrations in the presence or absence of antioxidants (Vit C or NAC). ROSup was used as the positive control. The cells were incubated with 25 μM DCFH-DA at 37 $^{\circ}\text{C}$ for 30 min, and the mean fluorescence intensity (MFI) was quantified using flow cytometry. Vit C: vitamin C; NAC: N-acetyl-L-cysteine.

red fluorescence was decreased in a dose-dependent manner compared to the untreated cells, which suggested that AgNPs could cause the losses of MMP. To further elucidate the role of AgNPs-induced ROS on mitochondrial damage, cells were incubated with AgNPs after the pretreatment with the antioxidants. The results showed that the mitochondrial damage could be completely abrogated in the presence of NAC while pretreatment of Vit C could partially rescue the losses of MMP.

3.5. Induction of apoptosis by AgNPs

It is well established that the generation or external addition of ROS could cause cell death by two distinct pathways, either apoptosis or necrosis [48]. Annexin V-FLOUS/PI assay was carried out to evaluate the extent and mode of cell death. The results indicated that AgNPs exposure could lead to apoptosis, mainly late apoptosis in SHI-1 cells (Fig. 7A and B), and the level of apoptosis was enhanced with the increased exposure dose (Data not shown). This apoptosis effect could be completely prevented by pretreatment with NAC but

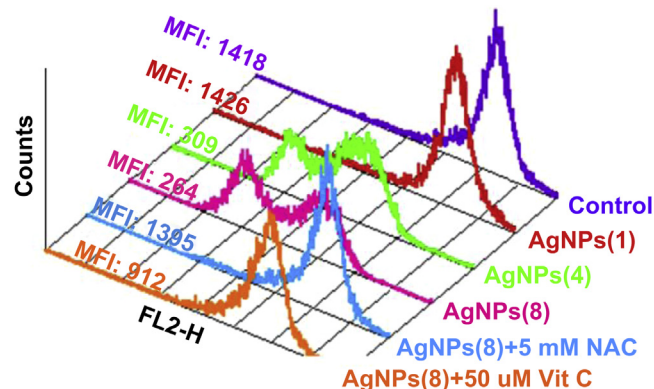


Fig. 6. Effect of AgNPs (11 nm) on mitochondrial membrane potential in the presence or absence of antioxidants (Vit C or NAC) for 24 h. After AgNPs-treatment, SHI-1 cells were stained with JC-1 and the intensity of red fluorescence of the stained cells was detected by flow cytometry. Red fluorescence was detected in FL2-H channel, the mean fluorescence intensity (MFI) of each sample was indicated as well.

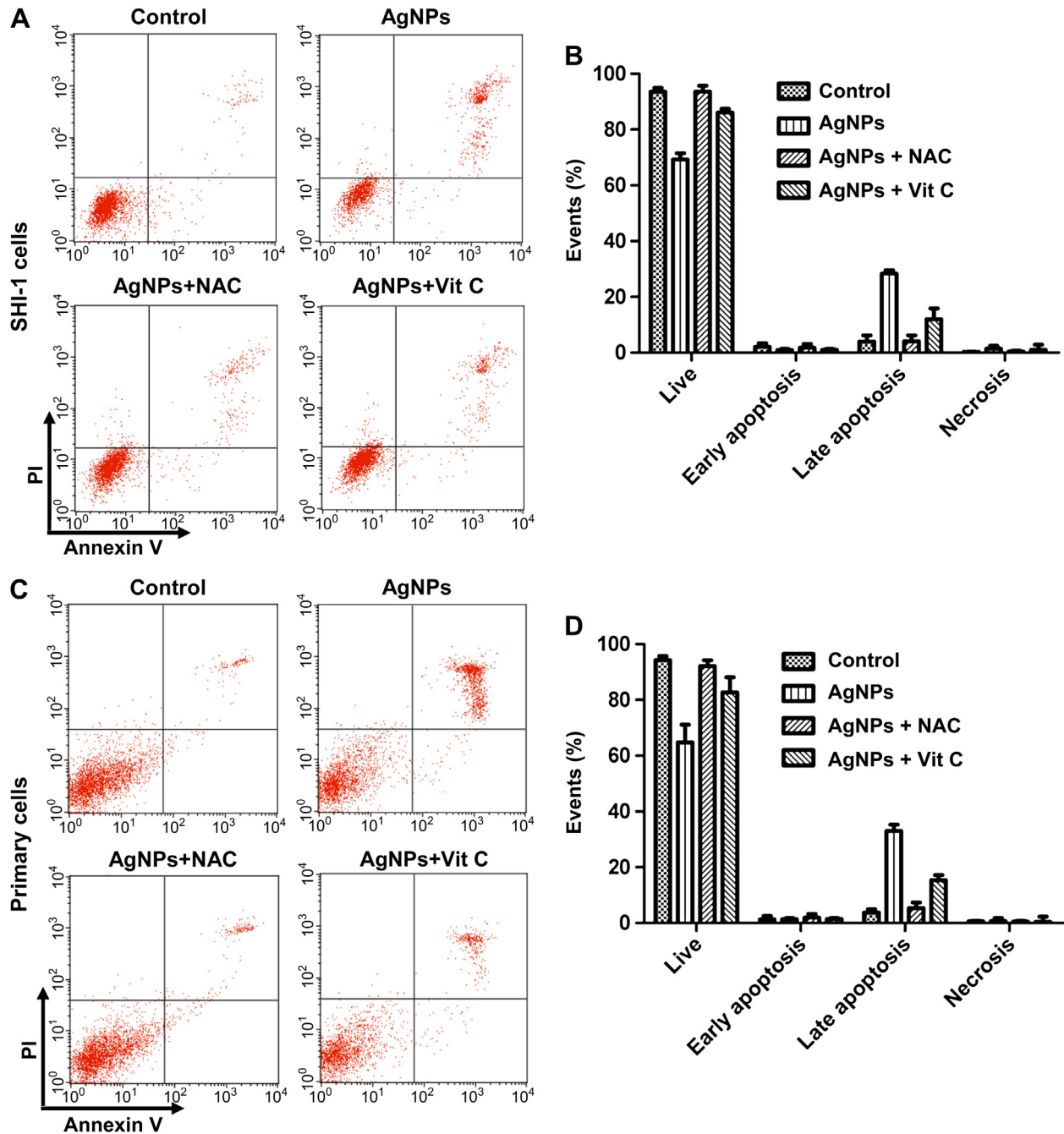


Fig. 7. Effect of AgNPs (11 nm, 8 $\mu\text{g}/\text{mL}$) on apoptosis in the presence or absence of antioxidants (Vit C or NAC) for 24 h. (A & B) The representative images and summaries of apoptosis of SHI-1 cells induced by AgNPs exposure were presented. (C & D) The representative images and summaries of apoptosis of the primary AML cells ($n = 3$) induced by AgNPs were presented.

not Vit C (Fig. 7A and B). Similar results were also confirmed in several clinical isolates of AML patients (Fig. 7C and D).

3.6. DNA damage caused by AgNPs

ROS are highly reactive and result in oxidative damage, which are considered to be the major source of spontaneous damage to DNA [49]. Several studies have reported that AgNPs could cause DNA damage [50,51]. To further investigate whether AgNPs brought about DNA damage, AML cells were tested for double-strand breaks (DSBs) in DNA by confocal microscopy. Confocal images of untreated and treated cells were shown in Fig. 8. The nuclei were stained blue with Hoechst 33342 and DSBs were indicated by bright

green FITC fluorescence foci. DSBs were seen in SHI-1 cells treated with AgNPs but not in untreated cells. Cells pretreated with NAC showed no DSBs, while DNA DSBs were still seen in cells pretreated with Vit C although the proportion of cells with DNA damage was decreased compared with the cells treated with AgNPs alone (Fig. 8A). Importantly, similar results were obtained with the cells from AML patients as well (Fig. 8B).

3.7. Both ROS and silver ions played important roles in the cytotoxic effect of AgNPs

Although a number of studies have documented the toxicities of AgNPs in variety of cells and organisms, the mechanisms

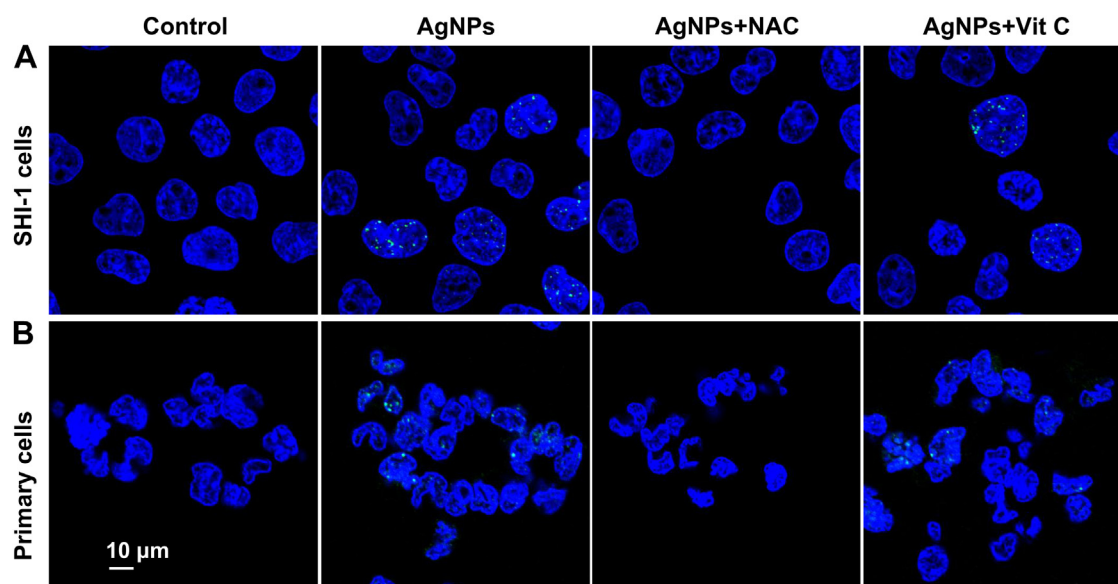


Fig. 8. Confocal images of DNA damage induced by AgNPs (11 nm, 8 µg/mL) in the presence or absence of antioxidants (Vit C or NAC) measured using the expression of phospho-H2AX. The cells' nuclei were stained with Hoechst 33342 (blue), and the expression of phospho-H2AX was stained with FITC (green). (A) The representative images of SHI-1 cells induced by AgNPs exposure were presented. (B) Similar experiments were done with cells obtained from 3 individual AML patients as well, and the representative images were shown. (For interpretation of the references to color in this figure legend, the reader is referred to the web version of this article.)

underlying AgNPs toxicity have not been clearly determined and a pivotal question is whether the toxicity is owing to nanoparticle itself or silver ions released from AgNPs. A large number of investigators have reported that cytotoxicity, DNA damage and apoptosis induced by AgNPs were through membrane peroxidation, ROS and oxidative stress [28,29]. For example, AgNPs could disrupt the mitochondrial respiratory chain, cause the accumulation of ROS, and even induce DNA damage in human lung fibroblast cells (IMR-90) and glioblastoma cells (U251). Our results confirmed the pivotal role of ROS as a mechanism of AgNPs-induced toxicity in AML cells. However, the enhancement of ROS was not only the mechanism underlying AgNPs toxicity. As described in results above, Vit C (50 µM) could not completely prevent the MMP change, DNA damage and apoptosis, though it could completely reverse ROS induced by AgNPs. Meanwhile, NAC (5 mM) could not only completely reverse the increase of ROS, but also completely prevented the losses of MMP, DNA damage and apoptosis. In addition to its role as an antioxidant, NAC could also serve as a silver ion chelator [33]. Therefore, we reasoned that ionic silver release played a role in AgNPs-mediated cytotoxicity in AML cells. As a matter of fact, a few studies also suggests that AgNPs act as a "Trojan horse", bypassing typical barriers and then releasing silver ions that damage cell machinery [52,53]. Furthermore, it has been reported that the drastic increase in intracellular ROS level could be detected during exposure to AgNPs and silver ions and the toxicity of silver ions is much higher than that of PVP-coated AgNPs in THP-1 cells [21]. Our results also indicated that silver ions could damage mitochondria, induce ROS production, and ultimately led to DNA damage and late apoptosis in SHI-1 cells (Fig. 9). Similar to the results of AgNPs, both Vit C and NAC reversed ROS, however, only NAC could completely protect the cells from DNA damage and apoptosis induced by silver ions. Interestingly, when treated with the same amount of total silver (1 µg/mL), cells exposed to AgNPs showed a similar level of ROS production to those treated with silver ions, however, silver ions displayed much higher toxicity than AgNPs (Fig. 9 and Fig. S1), suggesting that silver ion had other cytotoxic mechanism

independent of ROS, which was consistent with the rescue of cytotoxic effect by NAC.

Earlier studies have demonstrated the release of silver ions from AgNPs under abiotic conditions in water or simple buffers [54–56]. The dissolution of AgNPs to silver ions is an oxidation reaction. It is reported that the rate of intracellular oxidation of AgNPs is higher compared with dissolution in water, which may be attributed to high intracellular oxygen tension due to respiration and free radical production [55,57]. A customized protocol of cloud point extraction for separation of AgNPs and silver ions has been recently established, which could successfully quantify AgNPs and silver ions in mammalian cells. Their results have documented that about 10.3% and 17.9% of Ag as silver ions existed in HepG2 cells and MEL cells treated with PVP-coated AgNPs for 24 h [30,58]. Additionally, Singh et al. have demonstrated the accumulation of silver ions in lysosomes using a technique based on their accumulation in lysosomes followed by their conversion to visible precipitates in RAW 264.7 cells [31]. Biological effects of nanoparticles are closely related to their cellular transportation and intracellular location. It has been reported that PVP-coated AgNPs could enter the cells via endocytosis and localized in lysosomes [24,59]. NPs can induce ROS production directly once they are exposed to the acidic environment of lysosomes [60]. ROS contain superoxide anions ($O_2^{\cdot-}$), hydroxyl radicals ($\cdot OH$) and hydrogen peroxide (H_2O_2). AgNPs can induce $\cdot OH$ production in the presence of H_2O_2 in the acidic environment [61]. $\cdot OH$ is generally considered as one of the most toxic ROS species and is able to oxidize almost all the cellular components [62]. Both AgNPs and silver ions escaped from lysosomes could interfere with mitochondrial activity and further induce the increase of intracellular ROS. In turn, ROS could promote the oxidation of AgNPs and further significantly lead to the enhancement of the liberation of silver ions from AgNPs especially in the lysosomes due to the lower pH there [31,61,63]. Thus, AgNPs would cause a sustained ROS production and release of silver ions once inside cells, and ultimately result in a series of adverse effects on these cells.

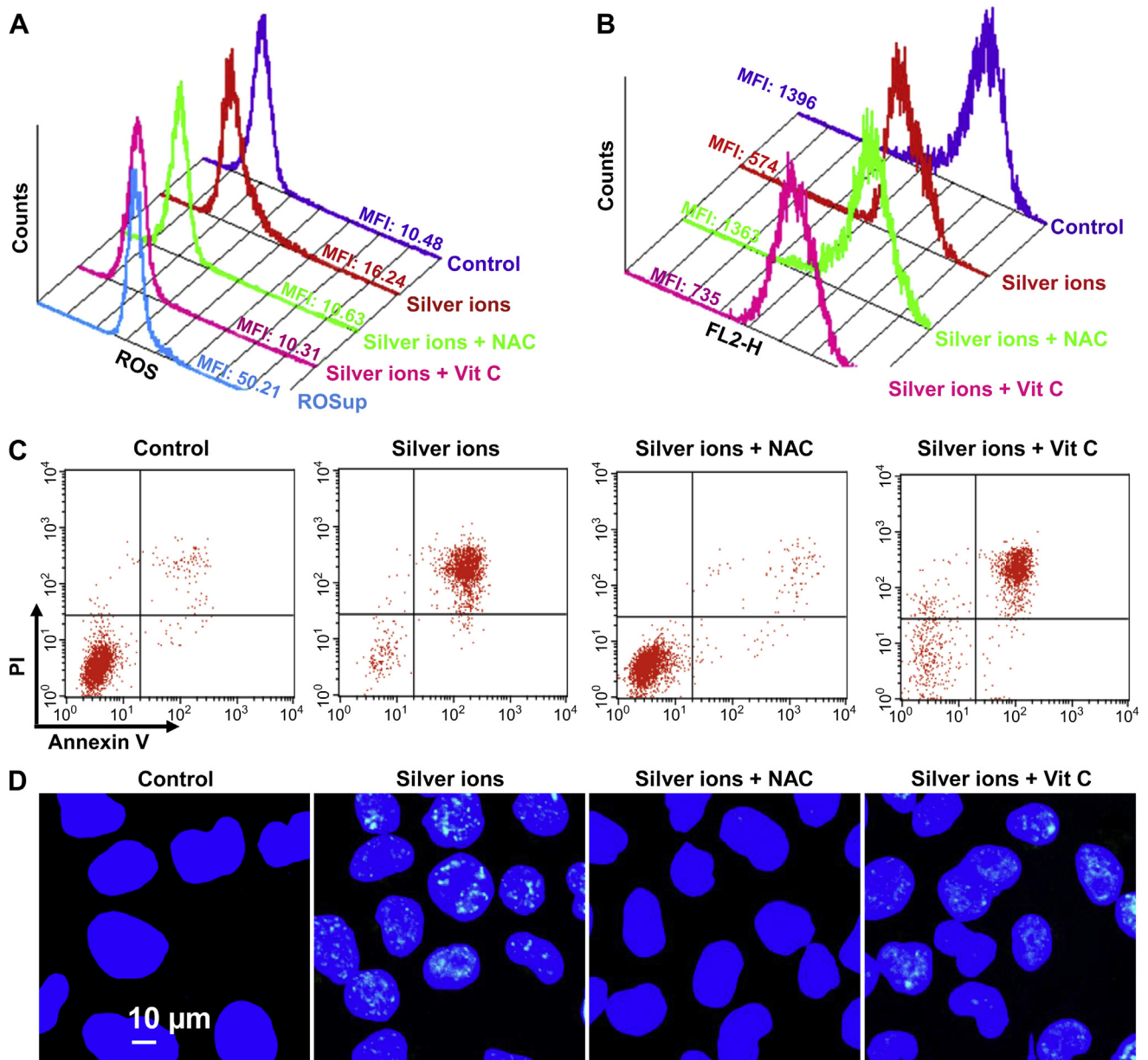


Fig. 9. Effect of silver ions (1 μ g/mL) on SHI-1 cells. (A) The cells were incubated with DCFH-DA before their treatment with silver ions with or without Vit C or NAC, and then the mean fluorescence intensity (MFI) was measured using flow cytometry. (B) After silver ion-treatment, cells were stained with JC-1 and the MFI was measured with flow cytometry. (C) Cellular apoptosis of various silver ion-treated cells was detected with Annexin V-FLOUS and PI co-staining. (D) DNA damage (indicated as the expression of phospho-H2AX, green) of various silver ion-treated cells was detected with confocal microscopy, and the nuclei were stained with Hoechst 33342 (blue). (For interpretation of the references to color in this figure legend, the reader is referred to the web version of this article.)

4. Conclusion

In this report, we demonstrated the PVP-coated AgNPs with various sizes had anti-leukemia effect against multiple human AML cell lines and primary isolates from AML patients; and the cytotoxic effect against AML cells was stronger than that against normal hematopoietic cells. We also explored the mechanism for AgNPs to inhibit the growth of AML cells, and our data supported a model in which both the generation of ROS and the release of silver ions were important for their cytotoxic effect. These data might provide a novel approach for the treatment of the disease in the future.

Conflict of interest

These authors declare no conflict of interest.

Acknowledgments

This work was supported by the grants from the National Key Basic Research Program of China (Nos. 2011CB933503 & 2011CB933501), the National Natural Science Foundation of China (NSFC, 61127002, 51201034, 31200757), the Special Project on Development of National Key Scientific Instruments and Equipment of China (2011YQ03013403), the Natural Science Foundation

of Jiangsu Province in China (BK2011036), the Graduate Research and Innovation Program of Jiangsu Province in China (CXZZ-0172), and a project funded by the Priority Academic Program Development of Jiangsu Higher Education Institutions (PAPD).

Appendix A. Supplementary data

Supplementary data related to this article can be found at <http://dx.doi.org/10.1016/j.biomaterials.2013.07.015>.

References

- [1] Bonnet D, Dick JE. Human acute myeloid leukemia is organized as a hierarchy that originates from a primitive hematopoietic cell. *Nat Med* 1997;3(7):730–7.
- [2] Cheson BD, Cassileth PA, Head DR, Schiffer CA, Bennett JM, Bloomfield CD, et al. Report of the National Cancer Institute-sponsored workshop on definitions of diagnosis and response in acute myeloid leukemia. *J Clin Oncol* 1990;8(5):813–9.
- [3] Robak T, Wierzbowska A. Current and emerging therapies for acute myeloid leukemia. *Clin Ther* 2009;31(2):2349–70.
- [4] Johnston HJ, Hutchison G, Christensen FM, Peters S, Hankin S, Stone V. A review of the in vivo and in vitro toxicity of silver and gold particulates: particle attributes and biological mechanisms responsible for the observed toxicity. *Crit Rev Toxicol* 2010;40(4):328–46.
- [5] Alarcon EI, Udekwi K, Skog M, Pacioni NL, Stampelcoskie KG, Gonzalez-Bejar M, et al. The biocompatibility and antibacterial properties of collagen-stabilized, photochemically prepared silver nanoparticles. *Biomaterials* 2012;33(19):4947–56.
- [6] Huang Z, Jiang X, Guo D, Gu N. Controllable synthesis and biomedical applications of silver nanomaterials. *J Nanosci Nanotechnol* 2011;11(11):9395–408.
- [7] Panacek A, Kolar M, Vecerova R, Prucek R, Soukupova J, Krystof V, et al. Antifungal activity of silver nanoparticles against *Candida* spp. *Biomaterials* 2009;30(31):6333–40.
- [8] Elechiguerra JL, Burt JL, Morones JR, Camacho-Bragado A, Gao X, Lara HH, et al. Interaction of silver nanoparticles with HIV-1. *J Nanobiotechnol* 2005;3:6.
- [9] Kalishwaralal K, BarathManiKanth S, Pandian SR, Deepak V, Gurunathan S. Silver nanoparticles impede the biofilm formation by *Pseudomonas aeruginosa* and *Staphylococcus epidermidis*. *Colloids Surf B Biointerfaces* 2010;79(2):340–4.
- [10] Wong KK, Cheung SO, Huang L, Niu J, Tao C, Ho CM, et al. Further evidence of the anti-inflammatory effects of silver nanoparticles. *ChemMedChem* 2009;4(7):1129–35.
- [11] Tian J, Wong KK, Ho CM, Lok CN, Yu WY, Che CM, et al. Topical delivery of silver nanoparticles promotes wound healing. *ChemMedChem* 2007;2(1):129–36.
- [12] Shrivastava S, Bera T, Singh SK, Singh G, Ramachandrarao P, Dash D. Characterization of antiplatelet properties of silver nanoparticles. *ACS Nano* 2009;3(6):1357–64.
- [13] Ragaseema VM, Unnikrishnan S, Kalliyana Krishnan V, Krishnan LK. The antithrombotic and antimicrobial properties of PEG-protected silver nanoparticle coated surfaces. *Biomaterials* 2012;33(11):3083–92.
- [14] Jun BH, Noh MS, Kim J, Kim G, Kang H, Kim MS, et al. Multifunctional silver-embedded magnetic nanoparticles as SERS nanoprobes and their applications. *Small* 2010;6(1):119–25.
- [15] Mahmood M, Casciano DA, Mocan T, Iancu C, Xu Y, Mocan L, et al. Cytotoxicity and biological effects of functional nanomaterials delivered to various cell lines. *J Appl Toxicol* 2010;30(1):74–83.
- [16] Gurunathan S, Lee KJ, Kalishwaralal K, Sheikpranbabu S, Vaidyanathan R, Eom SH. Antiangiogenic properties of silver nanoparticles. *Biomaterials* 2009;30(31):6341–50.
- [17] Nallathamby PD, Xu XH. Study of cytotoxic and therapeutic effects of stable and purified silver nanoparticles on tumor cells. *Nanoscale* 2010;2(6):942–52.
- [18] Sriram MI, Kanth SB, Kalishwaralal K, Gurunathan S. Antitumor activity of silver nanoparticles in Dalton's lymphoma ascites tumor model. *Int J Nanomedicine* 2010;5:753–62.
- [19] Sanpui P, Chattopadhyay A, Ghosh SS. Induction of apoptosis in cancer cells at low silver nanoparticle concentrations using chitosan nanocarrier. *ACS Appl Mater Interfaces* 2011;3(2):218–28.
- [20] Liu J, Zhao Y, Guo Q, Wang Z, Wang H, Yang Y, et al. TAT-modified nano-silver for combating multidrug-resistant cancer. *Biomaterials* 2012;33(26):6155–61.
- [21] Foldbjerg R, Olesen P, Hougaard M, Dang DA, Hoffmann HJ, Autrup H. PVP-coated silver nanoparticles and silver ions induce reactive oxygen species, apoptosis and necrosis in THP-1 monocytes. *Toxicol Lett* 2009;190(2):156–62.
- [22] Eom HJ, Choi J. p38 MAPK activation, DNA damage, cell cycle arrest and apoptosis as mechanisms of toxicity of silver nanoparticles in Jurkat T cells. *Environ Sci Technol* 2010;44(21):8337–42.
- [23] Rahban M, Divsalar A, Saboury AA, Golestani A. Nanotoxicity and spectroscopy studies of silver nanoparticle: calf thymus DNA and K562 as targets. *J Phys Chem C* 2010;114(13):5798–803.
- [24] Guo D, Zhao Y, Zhang Y, Wang Q, Huang Z, Ding Q, et al. The cellular uptake and cytotoxic effect of silver nanoparticles on chronic myeloid leukemia cells. *J Biomed Nanotechnol* 2013. in press.
- [25] Thombre R, Mehta S, Mohite J, Jaisinghani P. Synthesis of silver nanoparticles and its cytotoxic effect against THP-1 cancer cell line. *Int J Pharma Bio Sci* 2013;4(1):184–92.
- [26] AshaRani PV, Low Kah Mun G, Hande MP, Valiyaveetil S. Cytotoxicity and genotoxicity of silver nanoparticles in human cells. *ACS Nano* 2009;3(2):279–90.
- [27] Carlson C, Hussain SM, Schrand AM, Braydich-Stolle LK, Hess KL, Jones RL, et al. Unique cellular interaction of silver nanoparticles: size-dependent generation of reactive oxygen species. *J Phys Chem B* 2008;112(43):13608–19.
- [28] Lim DH, Jang J, Kim S, Kang T, Lee K, Choi IH. The effects of sub-lethal concentrations of silver nanoparticles on inflammatory and stress genes in human macrophages using cDNA microarray analysis. *Biomaterials* 2012;33(18):4690–9.
- [29] Ahamed M, AlSalhi MS, Siddiqui MKJ. Silver nanoparticle applications and human health. *Clin Chim Acta* 2010;411(23–24):1841–8.
- [30] Wang Z, Liu S, Ma J, Qu G, Wang X, Yu S, et al. Silver nanoparticles induced RNA polymerase-silver binding and RNA transcription inhibition in erythroid progenitor cells. *ACS Nano* 2013;7(5):4171–86.
- [31] Singh RP, Ramarao P. Cellular uptake, intracellular trafficking and cytotoxicity of silver nanoparticles. *Toxicol Lett* 2012;213(2):249–59.
- [32] Beer C, Foldbjerg R, Hayashi Y, Sutherland DS, Autrup H. Toxicity of silver nanoparticles – nanoparticle or silver ion? *Toxicol Lett* 2012;208(3):286–92.
- [33] Yang XY, Gondikas AP, Marinakos SM, Auffan M, Liu J, Hsu-Kim H, et al. Mechanism of silver nanoparticle toxicity is dependent on dissolved silver and surface coating in *Caenorhabditis elegans*. *Environ Sci Technol* 2012;46(2):1119–27.
- [34] Guo D, Zhang X, Huang Z, Zhou X, Zhu L, Zhao Y, et al. Comparison of cellular responses across multiple passage numbers in Ba/F3-BCR-ABL cells induced by silver nanoparticles. *Sci China Life Sci* 2012;55(10):898–905.
- [35] Li L, Sun J, Li X, Zhang Y, Wang Z, Wang C, et al. Controllable synthesis of monodispersed silver nanoparticles as standards for quantitative assessment of their cytotoxicity. *Biomaterials* 2012;33(6):1714–21.
- [36] D'Souza AJ, Schowen RL, Topp EM. Polyvinylpyrrolidone-drug conjugate: synthesis and release mechanism. *J Control Release* 2004;94(1):91–100.
- [37] Kodaira H, Tsutsumi Y, Yoshioka Y, Kamada H, Kaneda Y, Yamamoto Y, et al. The targeting of anionized polyvinylpyrrolidone to the renal system. *Biomaterials* 2004;25(18):4309–15.
- [38] Liu X, Xu Y, Wu Z, Chen H. Poly(N-vinylpyrrolidone)-modified surfaces for biomedical applications. *Macromol Biosci* 2013;13(2):147–54.
- [39] Ma H, Huang S, Feng X, Zhang X, Tian F, Yong F, et al. Electrochemical synthesis and fabrication of gold nanostructures based on poly(N-vinylpyrrolidone). *ChemPhysChem* 2006;7(2):333–5.
- [40] Wang H, Qiao X, Chen J, Wang X, Ding S. Mechanisms of PVP in the preparation of silver nanoparticles. *Mater Chem Phys* 2005;94(2–3):449–53.
- [41] Farrag M, Thämer M, Tschurl M, Bürgi T, Heiz U. Preparation and spectroscopic properties of monolayer-protected silver nanoclusters. *J Phys Chem C* 2012;116(14):8034–43.
- [42] Wu J, Sun J, Xue Y. Involvement of JNK and P53 activation in G2/M cell cycle arrest and apoptosis induced by titanium dioxide nanoparticles in neuron cells. *Toxicol Lett* 2010;199(3):269–76.
- [43] Zhao F, Zhao Y, Liu Y, Chang X, Chen C. Cellular uptake, intracellular trafficking, and cytotoxicity of nanomaterials. *Small* 2011;7(10):1322–37.
- [44] Chang-Liu CM, Woloschak GE. Effect of passage number on cellular response to DNA-damaging agents: cell survival and gene expression. *Cancer Lett* 1997;113(1–2):77–86.
- [45] Wang K, Shindoh H, Inoue T, Horii I. Advantages of in vitro cytotoxicity testing by using primary rat hepatocytes in comparison with established cell lines. *J Toxicol Sci* 2002;27(3):229–37.
- [46] Piao MJ, Kang KA, Lee IK, Kim HS, Kim S, Choi JY, et al. Silver nanoparticles induce oxidative cell damage in human liver cells through inhibition of reduced glutathione and induction of mitochondria-involved apoptosis. *Toxicol Lett* 2011;201(1):92–100.
- [47] Austin LA, Kang B, Yen CW, El-Sayed MA. Plasmonic imaging of human oral cancer cell communities during programmed cell death by nuclear-targeting silver nanoparticles. *J Am Chem Soc* 2011;133(44):17594–7.
- [48] Rytter SW, Kim HP, Hoetzel A, Park JW, Nakahira K, Wang X, et al. Mechanisms of cell death in oxidative stress. *Antioxid Redox Signal* 2007;9(1):49–89.
- [49] Cooke MS, Evans MD, Dizdaroglu M, Lunec J. Oxidative DNA damage: mechanisms, mutation, and disease. *FASEB J* 2003;17(10):1195–214.
- [50] Austin LA, Kang B, Yen CW, El-Sayed MA. Nuclear targeted silver nanospheres perturb the cancer cell cycle differently than those of nanogold. *Bioconjug Chem* 2011;22(11):2324–31.
- [51] Ahamed M, Karns M, Goodson M, Rowe J, Hussain SM, Schlager JJ, et al. DNA damage response to different surface chemistry of silver nanoparticles in mammalian cells. *Toxicol Appl Pharmacol* 2008;233(3):404–10.
- [52] Park EJ, Yi J, Kim Y, Choi K, Park K. Silver nanoparticles induce cytotoxicity by a Trojan-horse type mechanism. *Toxicol In Vitro* 2010;24(3):872–8.
- [53] Pratsinis A, Hervella P, Leroux JC, Pratsinis SE, Sotiriou GA. Toxicity of silver nanoparticles in macrophages. *Small* 2013. in press.

- [54] Kittler S, Greulich C, Diendorf J, Koller M, Eppele M. Toxicity of silver nanoparticles increases during storage because of slow dissolution under release of silver ions. *Chem Mater* 2010;22(16):4548–54.
- [55] Liu J, Sonshine DA, Shervani S, Hurt RH. Controlled release of biologically active silver from nanosilver surfaces. *ACS Nano* 2010;4(11):6903–13.
- [56] Sotiriou GA, Pratsinis SE. Antibacterial activity of nanosilver ions and particles. *Environ Sci Technol* 2010;44(14):5649–54.
- [57] Navarro E, Piccapietra F, Wagner B, Marconi F, Kaegi R, Odzak N, et al. Toxicity of silver nanoparticles to *Chlamydomonas reinhardtii*. *Environ Sci Technol* 2008;42(23):8959–64.
- [58] Yu SJ, Chao JB, Sun J, Yin YG, Liu JF, Jiang GB. Quantification of the uptake of silver nanoparticles and ions to HepG2 cells. *Environ Sci Technol* 2013;47(7):3268–74.
- [59] Greulich C, Diendorf J, Simon T, Eggeler G, Eppele M, Koller M. Uptake and intracellular distribution of silver nanoparticles in human mesenchymal stem cells. *Acta Biomater* 2011;7(1):347–54.
- [60] Chang YN, Zhang MY, Xia L, Zhang J, Xing GM. The toxic effects and mechanisms of CuO and ZnO nanoparticles. *Materials* 2012;5(12):2850–71.
- [61] He WW, Zhou YT, Wamer WG, Boudreau MD, Yin JJ. Mechanisms of the pH dependent generation of hydroxyl radicals and oxygen induced by Ag nanoparticles. *Biomaterials* 2012;33(30):7547–55.
- [62] Yamakoshi Y, Umezawa N, Ryu A, Arakane K, Miyata N, Goda Y, et al. Active oxygen species generated from photoexcited fullerene (C₆₀) as potential medicines: O₂⁻ versus ¹O₂. *J Am Chem Soc* 2003;125(42):12803–9.
- [63] Liu J, Hurt RH. Ion release kinetics and particle persistence in aqueous nanosilver colloids. *Environ Sci Technol* 2010;44(6):2169–75.